科学通报 2020 年 第 65 卷 第 15 期: 1486 ~ 1495
论 文
《中国科学》杂志社
SCIENCE CHINA PRESS

右江盆地SEDEX金矿化类型的发现及意义

陈军[1,2], 黄智龙[1*], 杨瑞东[2], 杜丽娟[2], 苏文超[1], 郑禄林[3], 叶霖[1]

1. 中国科学院地球化学研究所, 矿床地球化学国家重点实验室, 贵阳 550081;
2. 贵州大学资源与环境工程学院, 贵阳 550025;
3. 贵州大学矿业学院, 贵阳 550025
* 联系人, E-mail: huangzhilong@vip.gyig.ac.cn

2019-12-16 收稿, 2020-02-19 修回, 2020-02-20 接受, 2020-05-13 网络版发表
国家自然科学基金(41802107)、贵州省科技计划(黔科合基础20191315号)和中国博士后科学基金(2019M653495)资助

摘要 卡林型金矿床是全球最重要的金矿化类型之一, 尽管已经有大量关于卡林型金矿床的研究成果发表, 但在巨量Au来源及成矿动力学背景方面仍存在很大的争议. 本研究以右江盆地中-上二叠统火山-沉积岩中新发现的自然Au为视角, 通过高精度的电子探针(EPMA)、纳米离子探针(NanoSIMS)和原位激光剥蚀(LA-ICP-MS)相结合, 进行自然Au的纳米矿物学、白铁矿原位硫同位素组成和微量元素分析. 结果显示, 中-上二叠统火山-沉积岩中发育大量具喷流沉积(SEDEX)特征的硫化物结核(白铁矿-黄铁矿-石英-重晶石), 自然Au主要以纳米级颗粒(1~5 μm)赋存在白铁矿裂隙中. EPMA分析显示, 自然Au中伴生Hg、Cu、Zn、Sb等低温成矿元素, 与卡林型金矿床成矿元素组合(Au-As-Hg-Sb±Cu±Zn)基本一致. 自然Au寄主矿物白铁矿具有较低的Co/Ni比值(平均0.12)、高的Ti含量(主要介于39~890 ppm (1 ppm = 1 μg/g), 部分测点Ti含量可达10000 ppm以上), 以及低的Cu(1~32 ppm)、As (1~920 ppm)、Zn(0~5 ppm)和Au(0~0.53 ppm)含量. 这种低Co/Ni比值和Ti富集特征表明, 白铁矿形成于沉积-成岩过程且与高Ti峨眉山玄武岩的喷发有关. 白铁矿δ^{34}S值介于20.30‰~34.29‰(平均25.86‰), 揭示其形成于一个硫酸盐较为封闭, 而H_2S较为开放的环境, 有机质参与的热化学硫酸盐还原作用(TSR)为大量硫化物的沉淀提供S. 以上这些证据显示与峨眉地幔柱有关的海底热水喷流导致低温成矿元素Au-Sb-Hg±Cu±Zn在中-晚二叠世火山-沉积岩中初步富集. 结合前人研究, 综合认为峨眉地幔柱活动可能为大规模的卡林型金矿化提供了成矿物质基础. 尽管峨眉地幔柱与卡林型金矿化之间的关系仍需进一步的研究, 但无疑本次的研究发现对重新审视二者之间的关系具有重要意义.

关键词 自然金, 喷流沉积(SEDEX), 峨眉山玄武岩, 卡林型金矿床, 右江盆地

卡林型金矿床是全球重要的金矿床类型之一, 大约提供了8%的Au金属量[1]. 卡林型金矿床一般在独特的构造单元内(如背斜、穹隆构造)呈密集产出, 形成极具经济价值的矿集区. 例如, 在美国内华达地区6×10^4 km^2的范围内探明了7971 t的Au金属量[2], 形成了一个世界级的"金成矿省". 同样, 位于我国"滇-黔-桂"地区的右江盆地是我国重要的卡林型成矿区, 发育众多的大型-超大型矿床, 目前已探明Au金属量约800 t[3]. 鉴于卡林型金矿床的经济价值和成矿特殊性, 国内外学者对卡林型矿床的成矿过程开展了大量研究, 并取得了诸多共识性的认识. 就右江盆地而言, 初步确定右江卡林型金矿床成矿时代集中在印支期(235~200 Ma[4,5])和燕山晚期(148~134 Ma[6~8]), 热液硫(S)主要来自岩浆(如水银洞超大型矿床[9])或者是岩浆硫和地层硫的混

引用格式: 陈军, 黄智龙, 杨瑞东, 等. 右江盆地SEDEX金矿化类型的发现及意义. 科学通报, 2020, 65: 1486–1495
Chen J, Huang Z L, Yang R D, et al. Discovery of SEDEX gold in the Youjiang basin, SW China: Implications for a new type Au mineralization (in Chinese). Chin Sci Bull, 2020, 65: 1486–1495, doi: 10.1360/TB-2019-0837

合[10]. 然而, 由于含Au矿物的复杂性和有争议的成矿年代, 巨量Au的来源及其成矿动力背景仍是一个亟待解决的科学问题.

近些年开展的"华南大规模低温成矿作用"研究[11]认为, 不同成矿区元素组合特征可能与基底岩石性质有关, 如右江盆地以Au-Sb-As-Hg为主, 湘中盆地以Au-Sb为主, 这些基底岩石可能提供了主要的成矿物质. 一般来讲, 在地层中要萃取如此巨大的金属量需要持久的、超具规模的热动力. 根据同位素示踪(S-H-O-C)信息以及地球物理证据, 推测成矿热驱动可能与隐伏岩浆有关[9,12]. 但是, 这种推测目前没有直接的证据予以支持. 最新研究显示, 右江盆地卡林型金矿床与峨眉地幔柱的活动存在成因联系. Zhu等人[13]基于对峨眉地幔柱热力学模型、右江盆地金矿化凝灰岩锆石SIMS U-Pb年代学和原位氧同位素分析, 认为由峨眉地幔柱形成的新生下地壳为一个潜在卡林Au储库. 这一认识引发了对地幔柱和卡林型金矿化相互关系的重新思考. 从目前的研究来看, 右江盆地卡林型金矿床Au的来源具有多来源特征(盆地变质基底、沉积地层、下地壳). 同样, 在美国内华达地区, 卡林型Au也存在多来源, 除与岩浆有关外, 泥盆系地层中的喷流沉积(SEDEX)成因Au也为后期(~40 Ma)大规模卡林型金矿化提供了部分成矿物质[14].

地幔柱是地球各圈层进行能量和物质交换的重要形式, 深部物质和能量向地表迁移, 影响着浅部地表系统、岩浆和热液成矿系统. 峨眉地幔柱不仅形成了大面积的峨眉山玄武岩喷发(~260 Ma), 同时在空间上和时间尺度上都影响着众多矿床(如Pb、Zn、Cu、Ti、V等)的形成[15]. 根据Ti的含量, 峨眉山玄武岩可分为高钛(TiO_2 > 2.5 wt.%)和低钛(TiO_2 < 2.5 wt.%)玄武岩. 右江盆地范围内的玄武岩主要为高Ti玄武岩, 其形成与岩浆演化晚期残余流体中Fe-Ti氧化物的结晶有关[16]. 在右江盆地成矿带, 普遍分布有一套与峨眉山玄武岩喷发的火山碎屑岩沉积建造, 因其别具特色的岩石组合, 以及含有金、锑、萤石、硫铁矿等矿产资源而备受地球科学界关注. 前人在金、锑矿床的研究中称之为"大厂层"[17]或者"构造蚀变体(SBT)"[18], 如泥堡、戈塘金矿床和晴隆锑矿床主要赋存于该层位(图1). 这套火山沉积碎屑岩被认为是在峨眉地幔柱活动前期由于盆地扩张引发的火山活动形成, 其成分主要由流纹岩和流纹质英安岩组成, 在"川-滇-黔"交接区域广泛分布, 其分布西起富源-盘县-普安-晴隆-关岭一线, 东至安龙-贞丰一线尖灭, 厚度变化主要介于5~30 m, 在横向上层位较为稳定, 最大厚度可达百米[18,19].

1 研究方法及结果

1.1 岩相学

本研究发现的自然Au剖面位于黔西南晴隆锑矿区范围内(25°40′22.1″N; 105°10′28.2″E), 剖面未受到明显的热液蚀变. 剖面沉积序列为: 茅口组生物碎屑灰岩→硅质岩(1.6 m)→铁锰质层(3 cm)→纹层状铁质黏土岩(2.4 m)→黑色泥岩(凝灰岩)(1~4 m)→沉凝灰岩→球状玄武岩→块状玄武岩(图2(a), (b)), 显示出火山-热水沉积序列特征. 在黑色泥岩(凝灰岩)段的中下部(图2(a)), 发育大量硫化物结核(图2(c)). 这些硫化物结核呈管柱状(图3(a)), 表面为疏松多孔状(图3(e)), 直径约6~8 cm(图2(c), 3(a)). 横断面呈环形构造, 核部仍然保留有喷流通道(图3(b)); 纵断面核部为块状、胶状黄铁矿, 边缘为放射状、针状白铁矿(图3(c)). 硫化物结核中主要由白铁矿、黄铁矿、黄铜矿、闪锌矿、石英, 以及少量的重晶石和有机质组成(图3(d), (f)). 在现代陆壳海底玄武岩金成矿区(如日本Higashi-Aogashima海底热液区), 火山泥和硫化物结核中可见大量的自然Au及其他金属硫化物[21]. 通过对比, 本研究发现的这些含Au硫化物结核不论是在矿物组成还是结构构造方面均与Higashi-Aogashima海底热液区硫化物类似. 这些特征表明, 这些含自然Au硫化物结核为海底喷流活动形成(SEDEX). 根据峨眉山玄武岩喷发机制[15], 其形成背景可能与中-晚二叠世峨眉地幔柱抬升引发的陆内伸展环境有关.

1.2 矿物学

自然Au主要以纳米级颗粒赋存在与有机质共生的白铁矿矿物裂隙中(图4). 电子探针面扫描分析显示(图5), 在自然Au颗粒中伴生Hg、Cu、Zn、Sb以及Co和Ni, 这种成矿元素组合(Au-Hg-Cu-Zn-Sb)暗示流体中除富集Au以外, Hg-Cu-Zn-Sb也直接来自含Au成矿流体, 与右江盆地卡林型金矿床的元素组合(Au-Sb-As-Hg±Cu±Zn)类似[3]. 然而不同的是, Co和Ni的富集暗示了这种自然Au的来源与卡林型矿化不同, 因为在右江盆地卡林型金矿床黄铁矿含Au热液环带中, Co和Ni含量较低, 一般小于200 ppm[9](1 ppm=1 μg/g, 下同). 值得一提的是, 在卡林型环带状黄铁矿的核部, Co和Ni呈现

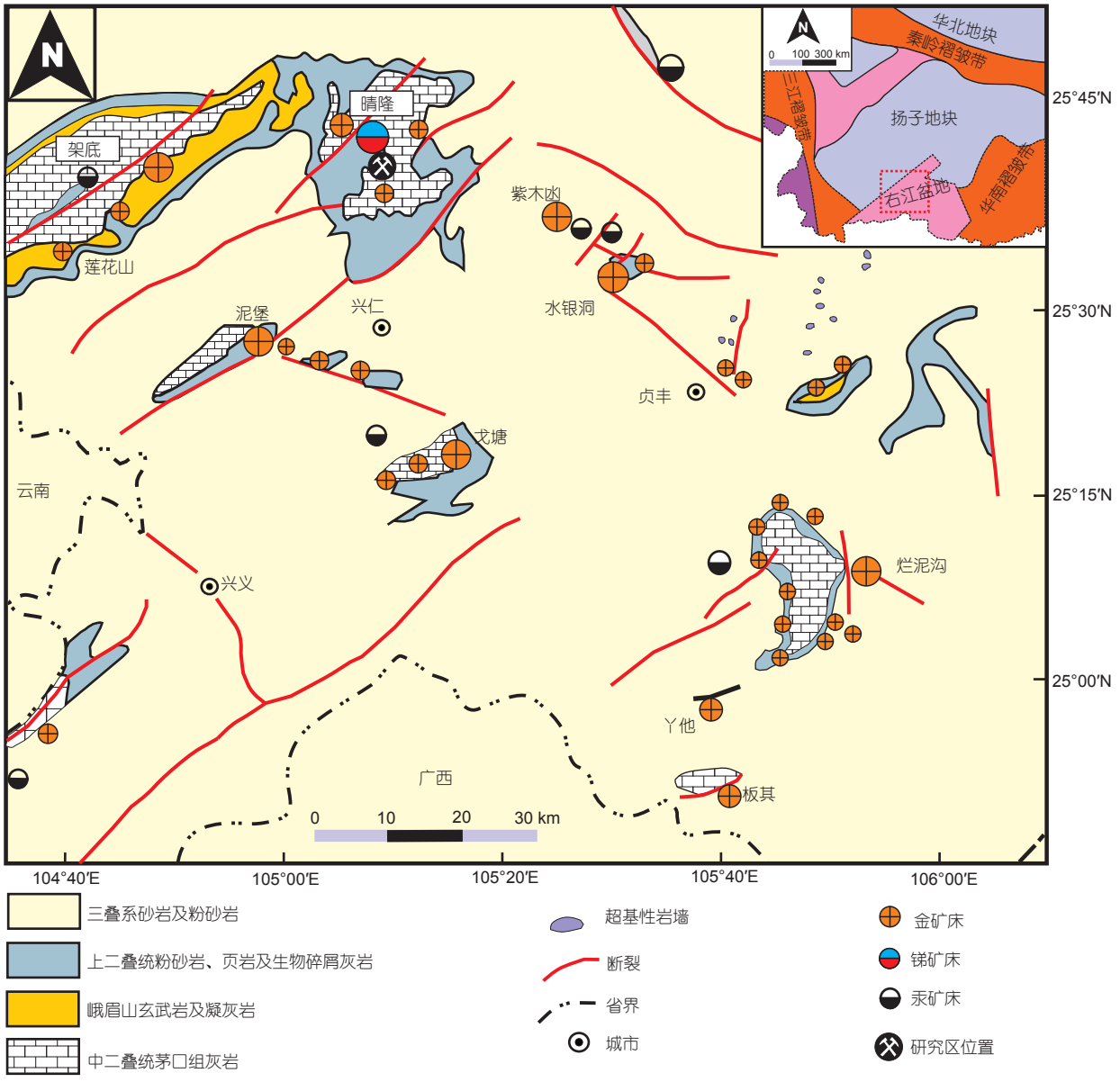

图 1 黔西南区域地质矿产图. 根据文献[20]修改

Figure 1 Regional geological sketch map of southwestern Guizhou. Modified from Ref. [20].

出明显的富集(Co平均=635 ppm; Ni平均=1328 ppm[9]). 前人研究一致认为, 这种富集Co和Ni的黄铁矿核部一般由沉积-成岩过程形成[3,9,22]. 由此可见, 本次发现的自然Au的形成不同于卡林Au矿化, 而可能与围岩的沉积-成岩过程有关. 但是, 元素组合的相似性则暗示自然Au与卡林Au之间存在潜在的继承关系.

1.3 硫化物原位微量元素

对自然Au寄主矿物进行LA-ICP-MS微量元素分析显示, Ti含量大多介于39~890 ppm(平均241 ppm), 但部分测点Ti含量可达10000 ppm以上, 暗示白铁矿中存在Ti矿物包体. 在前文已指出, 研究区峨眉山玄武岩为高钛玄武岩, 因此白铁矿中Ti的富集与峨眉山玄武岩的喷发有关. 除Ti之外, 其他微量元素Co(4~60 ppm)、Ni(3~539 ppm)、Cu(1~32 ppm)、As(1~920 ppm)、Zn(0~5 ppm)和Au(0~0.53 ppm)明显低于卡林型微量元素含量. 白铁矿Co/Ni比值平均为0.12(n=14), 明显不同于卡林型黄铁矿含Au热液环带的Co/Ni比值(≥1)[22], 这

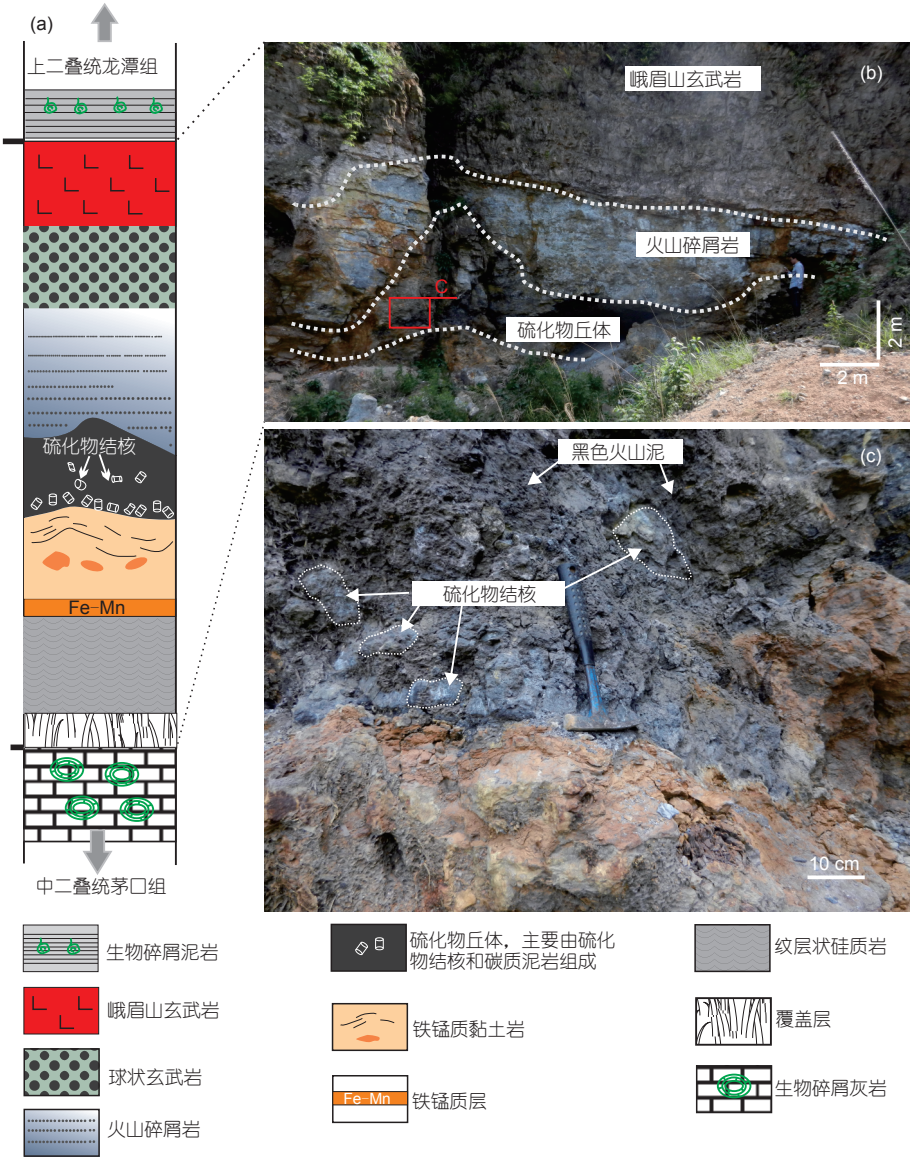

图 2 右江盆地晴隆锑矿区中-晚二叠世火山-沉积剖面序列. (a) 中二叠统茅口期至龙潭期火山-沉积序列柱状图; (b) 野外剖面图; (c) 硫化物结核剖面产出形态

Figure 2 The sedimentary sequences of volcanic-sedimentary rocks in the Middle-Late Permian, Qinglong district, Youjiang basin. (a) Histogram of volcanic-sedimentary rocks in the Middle Permian Maokou formation and Upper Longtan formation; (b) geological cross section of volcanic-sedimentary rocks; (c) occurrence of sulfide concretions in metalliferous sediments

种低Co/Ni比值的白铁矿属于成矿前期(沉积-成岩阶段)的产物[23].

1.4 硫同位素组成

白铁矿NanoSIMS硫同位素组成分析表明, 这些白铁矿明显富集重硫, δ^{34}S值介于20.30‰~34.29‰, 平均为25.86‰(n=11), 硫同位素分馏达13.99‰. 需要说明的是, 我们在这套火山-沉积岩中发现大量的有机质(如沥青)存在[17], 同样白铁矿与有机质也是紧密共生的(图6). 岩相学研究显示, 这些硫化物结核的形成与峨眉山玄武岩喷发时期的海底热水喷流活动有关. 在海底热水喷流条件下(温度>50°C), 细菌活动较弱, 但有利于热化学硫酸盐还原(TSR)作用, 而地层中的有机质充当了还原剂的角色. 目前针对晴隆地区"大厂层"的研究表明, 在峨眉山玄武岩喷发前期, 研究区处于一个局限的浅海盆地[24]. 在这种局限的环境下, 硫酸盐得不到持续

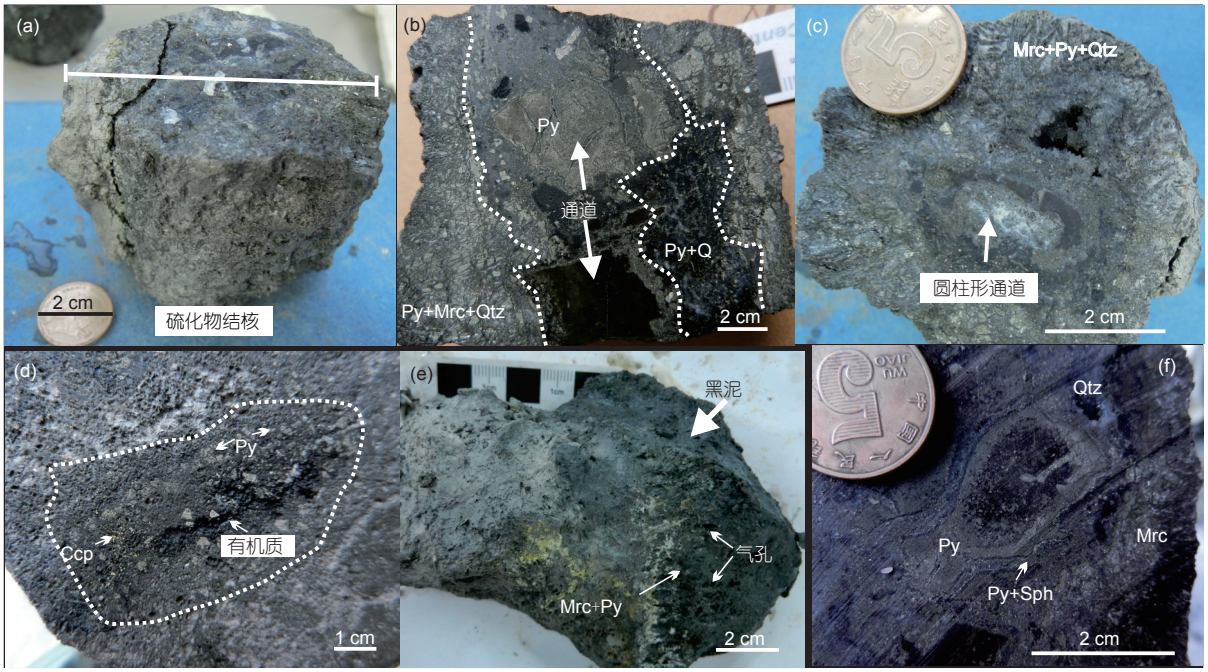

图 3 (网络版彩色)右江盆地中-晚二叠世火山-沉积岩中硫化物结核矿物组成及结构特征. (a) 硫化物结核; (b) 硫化物结核纵切面, 核部为粗粒黄铁矿, 边缘为放射状白铁矿; (c) 环状硫化物结核横切面; (d) 火山泥岩中有机质与细粒黄铁矿和黄铜矿共生; (e) 硫化物结核表面的黑色火山泥以及气孔; (f) 硫化物中的黄铁矿、闪锌矿和白铁矿. 矿物缩写: Py, 黄铁矿; Mrc, 白铁矿; Qtz, 石英; Ccp, 黄铜矿; Sph, 闪锌矿

Figure 3 (Color online) Minerals and structures of sulfide concretions in volcano-sedimentary rocks in the Middle-Late Permmian, Youjiang basin. (a) Sulfide concretions; (b) vertical section of concretions show that coarse-grained pyrite in core and radial marcasite in rim; (c) cyclic radial texture of cross section; (d) organic matter coexists with fine-grained pyrite and chalcopyrite; (e) black ash and vents in sulfide concretion surface; (f) pyrite, marcasite and sphalerite occur in sulfide concretion. Abbreviations: Py, pyrite; Mrc, marcasite; Qtz, quartz; Ccp, chalcopyrite; Sph, sphalerite

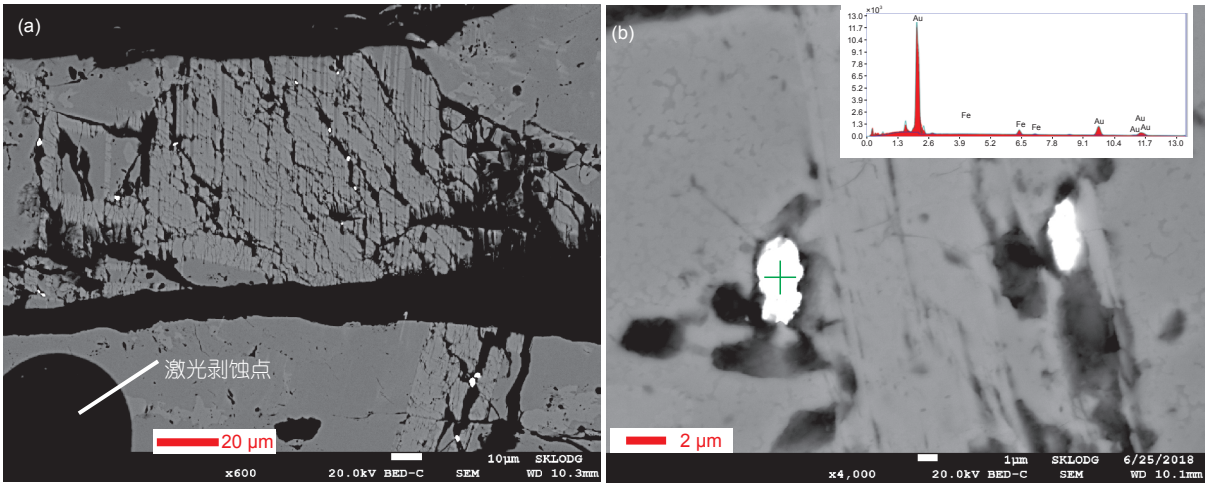

图 4 (网络版彩色)自然Au的赋存状态: 显示纳米Au赋存在白铁矿的裂隙中

Figure 4 (Color online) The occurrences of native gold show that these nano-scale gold particles occur in microfracture of marcasite

的补充, 而H_2S与金属离子结合形成大量硫化物, 致使形成一个近似的H_2S开放体系. 在这种硫酸盐相对封闭而H_2S相对开放的情况下, 硫化物的硫同位素组成会产生较大的分馏, 并且高于同时期的海水硫酸盐的硫同位素组成[25]. 因此, 这种$\delta^{34}S$值高于同时期海水(二叠纪海水$\delta^{34}S$约15‰)且分馏较大的S主要来自于硫酸盐的

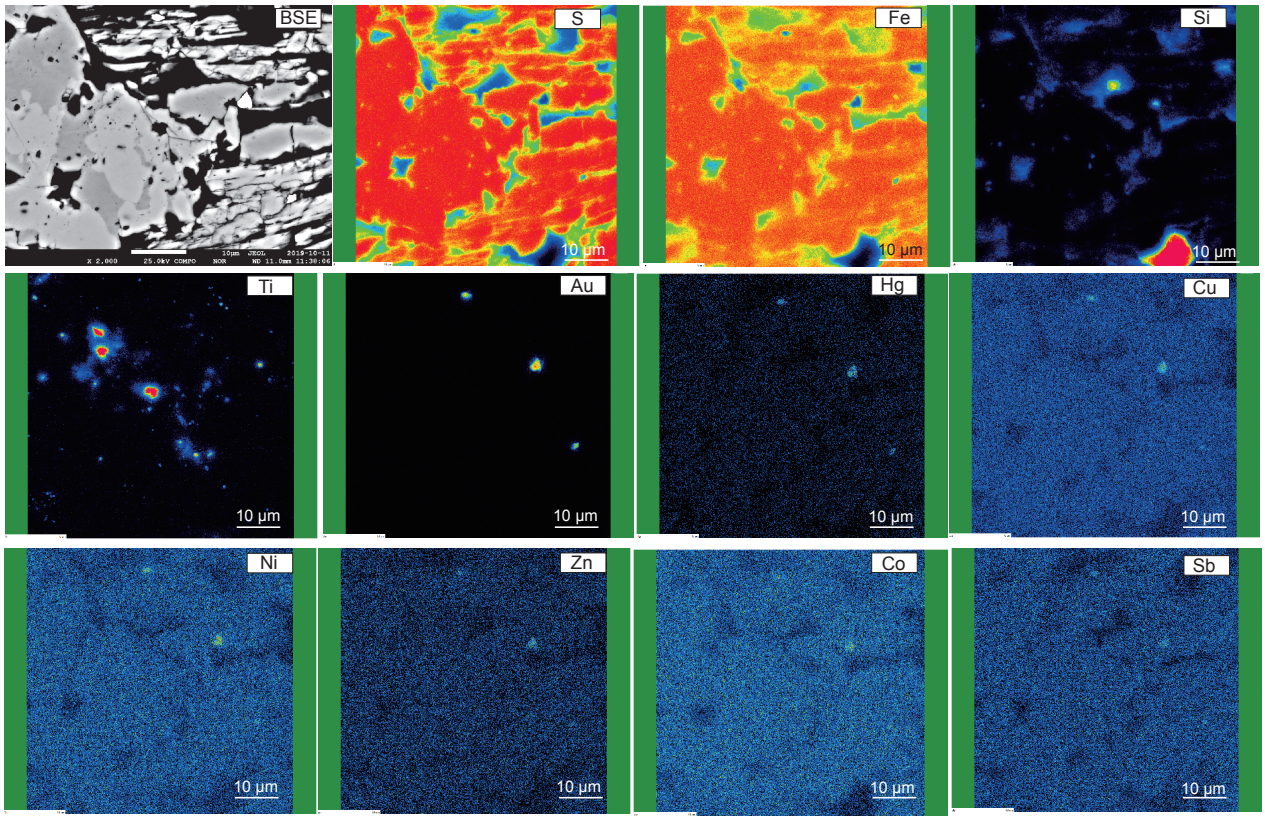

图 5 (网络版彩色)白铁矿中自然Au的背散射(BSE)和电子探针(EPMA)元素(S, Fe, Si, Ti, Au, Hg, Cu, Ni, Zn, Co, Sb)面扫描图
Figure 5 (Color online) The BSE and EPMA element (S, Fe, Si, Ti, Au, Hg, Cu, Ni, Zn, Co and Sb) mapping images of native gold particles in marcasite

热化学还原作用(TSR).

2 讨论

前人研究显示, 白铁矿的形成主要是在低pH(<2.5)和低温条件下(<220°C)由黄铁矿氧化和溶蚀形成并稳定存在[26,27]. 对白铁矿扫描电子显微镜分析显示(图5, BSE图), 白铁矿中元素存在不均一性, 这种成分不均一的白铁矿被认为由过饱和流体瞬间氧化或者是还原形成[28]. 事实上, 大多数金属的溶解度随着pH的降低而增加, 因此在白铁矿稳定的低pH条件下, 金属的活动性增强但不同金属之间的相容性较低[29], 这也导致了白铁矿中微量元素含量较低, 与本研究白铁矿微量元素低含量的结果一致. 自然Au的出现, 说明Au在流体中是过饱和的. 对于SEDEX硫化物来说, 当含矿流体进入海水时, 由于压力的急剧减少引起流体沸腾[21]. 这种流体释压沸腾进一步导致H_2S的逃逸, 致使流体瞬间氧化, 溶蚀黄铁矿形成白铁矿. 因此, 在流体过饱和的情况下, 瞬间的氧化非常有利于复杂成分白铁矿的形成[28], 同样这种沸腾作用也非常有利于自然Au的沉淀(如Higashi-Aogashima海底热液区[21]), 而微量元素(如Cu, As, Zn等)因具有高溶解度在白铁矿中少量沉淀. 另外, 刘家军等人[30]对黔西南卡林型金矿床容矿硅质岩的研究认为具有喷流沉积特征, 为本次含Au硫化物的SEDEX成因提供了佐证.

可以看出, 这种SEDEX成因自然Au的形成明显是不同于卡林型金矿床(如水银洞)的中高温(200~300°C)和中性流体条件[3]. 那么, SEDEX成因Au与卡林型Au之间存在什么关系呢? 在前人对卡林型金矿床的研究中, 虽然Au主要以不可见Au的形成存在[3,31], 但也不乏有自然Au的报道. 如在美国内华达卡林金成矿区发现SEDEX自然Au[14], 右江盆地卡林型金矿床最早(1991年)在板其金矿床就被发现有自然Au的存在[32], 之后在贵州水银洞金矿床也发现有少量纳米级的自然Au[33]. 最新研究认为, 除了不可见Au(Au^{1+})外, 纳米Au也可能是右江盆地卡林型金的赋存方式之一[22]. 前文指出, 本研究发现的SEDEX自然Au伴生有与卡林型类似的低

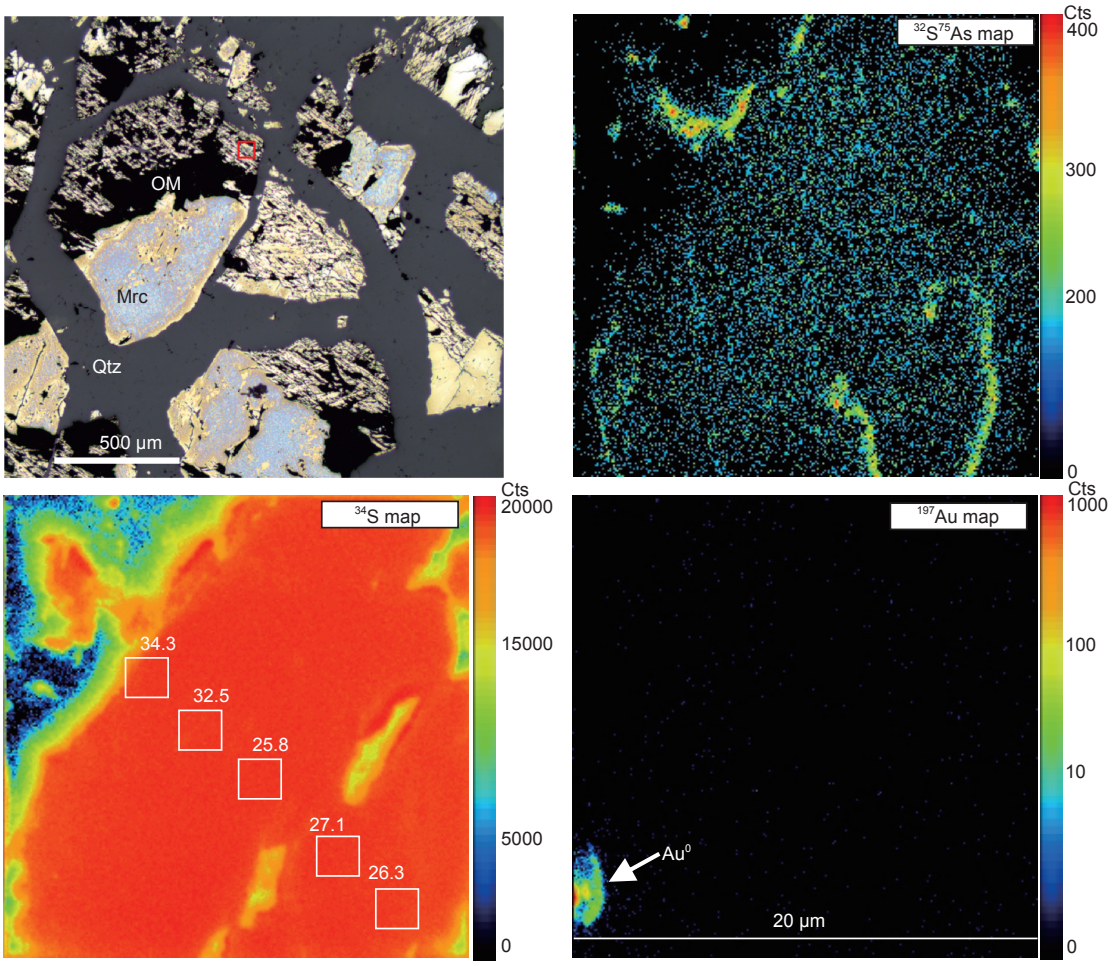

图 6 含自然Au白铁矿(Mrc)NanoSIMS元素($^{32}S^{75}As$、^{34}S和^{197}Au)面扫描图以及硫同位素组成分布图
Figure 6 NanoSIMS elemental maps of $^{32}S^{75}As$, ^{34}S, ^{197}Au and nanoscale-distribution of $\delta^{34}S$ values of Au-bearing marcasite

温元素组合(Au-Sb-As-Hg±Cu±Zn), 暗示两种类型矿化存在继承关系. 从成矿年代学来看, 这些SEDEX矿化时间约为260 Ma(峨眉山玄武岩年龄[16]), 而大规模的卡林金矿化时间为140 Ma[6~8]. 那么, SEDEX成矿元素(Au-Hg-Cu-Zn-Sb)是否受后期低温成矿事件的影响被重新活化而进入卡林型成矿系统? 其一, 根据卡林型金矿床的研究[2,3,9,10], 具有"核-边"结构的环带状黄铁矿为主要的载金矿物, "核"形成于沉积-成岩阶段以低微量元素(Au-As-Sb-Hg)为特征, 而"边"主要形成于热液阶段以富Au和As为特征. 其二, 含自然Au白铁矿的Co/Ni比值与卡林型含Au黄铁矿的"核"部Co/Ni比值接近, 揭示都为沉积-成岩期的产物. 最近, Xing等人[34]通过实验模拟研究证实, 当早期低品位的黄铁矿被后期多级流体反复改造时, 成矿元素会逐渐被迁移至热液环带中富集, 这也是形成大型金矿床的主要机制之一. 因此, 当这些具有低Co/Ni比值且含Au的白铁矿"核"被后期热液(~140 Ma[7])不断交代溶蚀时, 会发生元素由核部向边缘的迁移. 根据最新在热液环带中纳米Au的发现, 推测这些SEDEX自然Au(核部)通过粒内扩散机制进入了卡林成矿系统(热液环带). 因为在低温条件下, 高熔点的Au可以被低温的流体再次搬运[35,36].

3 结论

在右江盆地中-上二叠统火山-沉积岩中的自然Au, 为海底热水喷流的沉积成因(SEDEX), 其成矿动力背景与峨眉地幔柱活动有关. 这些SEDEX成因Au可能为后期(~140 Ma)大规模卡林型矿化提供了部分物质基础. 该研究为峨眉地幔柱与卡林型金矿化之间的关系提供了最直接的证据, 无疑对于研究二者之间的成矿关系具有重要意义.

参考文献

1 Muntean J L, Cline J S. Diversity of Carlin-style gold deposits. Rev Econ Geol, 2018, 20: 1–6
2 Muntean J L. The Carlin gold system: Applications to exploration in Nevada and beyond. Rev Econ Geol, 2018, 20: 39–88
3 Su W C, Dong W D, Zhang X C, et al. Carlin-type gold deposits in the Dian-Qian-Gui “Golden Triangle” of southwest China. Rev Econ Geol, 2018, 20: 157–185
4 Chen M, Mao J, Li C, et al. Re-Os isochron ages for arsenopyrite from Carlin-like gold deposits in the Yunnan-Guizhou-Guangxi “golden triangle”, southwestern China. Ore Geol Rev, 2015, 64: 316–327
5 Pi Q, Hu R, Xiong B, et al. *In situ* SIMS U-Pb dating of hydrothermal rutile: Reliable age for the Zhesang Carlin-type gold deposit in the golden triangle region, SW China. Miner Depos, 2017, 52: 1179–1190
6 Su W, Hu R, Xia B, et al. Calcite Sm-Nd isochron age of the Shuiyindong Carlin-type gold deposit, Guizhou, China. Chem Geol, 2009, 258: 269–274
7 Chen M H, Bagas L, Liao X, et al. Hydrothermal apatite SIMS Th-Pb dating: Constraints on the timing of low-temperature hydrothermal Au deposits in Nibao, SW China. Lithos, 2019, 324-325: 418–428
8 Zheng L L, Yang R D, Gao J B, et al. Quartz Rb-Sr isochron ages of two type orebodies from the Nibao Carlin-type gold deposit, Guizhou, China. Minerals, 2019, 399: 1–15
9 Xie Z, Xia Y, Cline J S, et al. Magmatic origin for sediment-hosted Au deposits, Guizhou Province, China: *In situ* chemistry and sulfur isotope composition of pyrites, Shuiyindong and Jinfeng Deposits. Econ Geol, 2018, 113: 1627–1652
10 Yan J, Hu R, Liu S, et al. NanoSIMS element mapping and sulfur isotope analysis of Au-bearing pyrite from Lannigou Carlin-type Au deposit in SW China: New insights into the origin and evolution of Au-bearing fluids. Ore Geol Rev, 2018, 92: 29–41
11 Hu R, Fu S, Huang Y, et al. The giant South China Mesozoic low-temperature metallogenic domain: Reviews and a new geodynamic model. J Asian Earth Sci, 2017, 137: 9–34
12 Hou L, Peng H, Ding J, et al. Textures and *in situ* chemical and isotopic analyses of pyrite, Huijiabao trend, Youjiang basin, China: Implications for paragenesis and source of sulfur. Econ Geol, 2016, 111: 331–353
13 Zhu J, Zhang Z C, Santosh M, et al. Carlin-style gold province linked to the extinct Emeishan plume. Earth Planet Sci Lett, 2019, doi: 10.1016/j.epsl.2019.115940
14 Emsbo P, Hutchinson R W, Hofstra A H, et al. Syngenetic Au on the Carlin trend: Implications for Carlin-type deposits. Geology, 1999, 27: 59
15 Xu Y K, Huang Z L, Zhu D, et al. Origin of hydrothermal deposits related to the Emeishan magmatism. Ore Geol Rev, 2014, 63: 1–8
16 Hou T, Zhang Z, Kusky T, et al. A reappraisal of the high-Ti and low-Ti classification of basalts and petrogenetic linkage between basalts and mafic-ultramafic intrusions in the Emeishan large igneous province, SW China. Ore Geol Rev, 2011, 41: 133–143
17 Chen J, Yang R D, Du L J, et al. Mineralogy, geochemistry and fluid inclusions of the Qinglong Sb-(Au) deposit, Youjiang basin (Guizhou, SW China). Ore Geol Rev, 2018, 92: 1–18
18 Liu J Z, Xia Y, Tao Y, et al. The relation between SBT and gold-antimony deposit metallogenesis and prospecting in southwest Guizhou (in Chinese). Guizhou Geol, 2014, 31: 268−271 [刘建中, 夏勇, 陶琰, 等. 贵州西南部SBT与金锑矿成矿找矿. 贵州地质, 2014, 31: 268−271]
19 Liu J Z, Wang Z P, Yang C F, et al. Metallogenic mechanism and model of gold and antimony deposits in southwest Guizhou (in Chinese). Acta Mineral Sin, 2015, 35(Suppl): 895−896 [刘建中, 王泽鹏, 杨成富, 等. 贵州西南部SBT分布区金锑矿成矿机制与成矿模式. 矿物学报, 2015, 35(Suppl): 895−896]
20 Li S, Xia Y, Liu J, et al. Geological and geochemical characteristics of the Baogudi Carlin-type gold district (Southwest Guizhou, China) and their geological implications. Acta Geochim, 2019, 38: 587–609
21 Iizasa K, Asada A, Mizuno K, et al. Native gold and gold-rich sulfide deposits in a submarine basaltic caldera, Higashi-Aogashima hydrothermal field, Izu-Ogasawara frontal arc, Japan. Miner Depos, 2019, 54: 117–132
22 Li J X, Hu R Z, Zhao C H, et al. Sulfur isotope and trace element compositions of pyrite determined by NanoSIMS and LA-ICP-MS: New constraints on the genesis of the Shuiyindong Carlin-like gold deposit in SW China. Miner Depos, 2019, doi: 10.1007/s00126-019-00929-w
23 Bralia A, Sabatini G, Troja F. A revaluation of the Co/Ni ratio in pyrite as geochemical tool in ore genesis problems. Miner Depos, 1979, 14: 353–374
24 Chen J, Yang R D, Zheng L L, et al. A research on the genesis of the conglomerate of Dachang Layer of Middle Permian in Qinglong, Guizhou (in Chinese). Geol Rev, 2014, 60: 1310–1322 [陈军, 杨瑞东, 郑禄林, 等. 贵州晴隆中二叠统大厂层砾岩成因研究. 地质论评, 2014, 60: 1310–1322]
25 Ohmoto H, Rye R O. Isotopes of sulfur and carbon. In: Barnes H L, ed. Geochemistry of Hydrothermal Ore Deposits. New York: Wiley, 1979. 509–567

26 Schieber J. Oxidation of detrital pyrite as a cause for Marcasite Formation in marine lag deposits from the Devonian of the eastern US. Deep-Sea Res Part II-Top Stud Oceanogr, 2007, 54: 1312–1326
27 Qian G, Xia F, Brugger J, et al. Replacement of pyrrhotite by pyrite and marcasite under hydrothermal conditions up to 220°C: An experimental study of reaction textures and mechanisms. Am Miner, 2011, 96: 1878–1893
28 Wu Y F, Evans K, Li J W, et al. Metal remobilization and ore-fluid perturbation during episodic replacement of auriferous pyrite from an epizonal orogenic gold deposit. Geochim Cosmochim Acta, 2019, 245: 98–117
29 Reed M H. Sulfide mineral precipitation from hydrothermal fluids. Rev Mineral Geochem, 2006, 61: 609–631
30 Liu J J, Liu J M, Gu X X, et al. Submarine sedimentary exhalative (SEDEX) origin of disseminated gold deposits in SW Guizhou (in Chinese). Chin Sci Bull, 1997, 42: 2126–2127 [刘家军, 刘建明, 顾雪祥, 等. 黔西南微细浸染型金矿床的喷流沉积成因. 科学通报, 1997, 42: 2126–2127]
31 Cline J S, Hofstra A H, Muntean J L, et al. Carlin-type gold deposits in Nevada, USA: Critical geologic characteristics and viable models. Econ Geol, 2005, 100th Anniversary Volume: 451–484
32 Chen F. The discovery of native gold in the Banqi gold deposit, SW China (in Chinese). Chin Sci Bull, 1991, 36: 1838 [陈丰. 板其金矿原生矿石中发现自然金. 科学通报, 1991, 36: 1838]
33 Su W, Xia B, Zhang H, et al. Visible gold in arsenian pyrite at the Shuiyindong Carlin-type gold deposit, Guizhou, China: Implications for the environment and processes of ore formation. Ore Geol Rev, 2008, 33: 667–679
34 Xing Y, Brugger J, Tomkins A, et al. Arsenic evolution as a tool for understanding formation of pyritic gold ores. Geology, 2019, 47: 335–338
35 Ciobanu C L, Cook N J, Damian F, et al. Gold scavenged by bismuth melts: An example from Alpine shear-remobilizates in the Highiş Massif, Romania. Mineral Petrol, 2006, 87: 351–384
36 Tooth B, Brugger J, Ciobanu C, et al. Modeling of gold scavenging by bismuth melts coexisting with hydrothermal fluids. Geology, 2008, 36: 815–818

Summary for “右江盆地SEDEX金矿化类型的发现及意义”

Discovery of SEDEX gold in the Youjiang basin, SW China: Implications for a new type Au mineralization

Jun Chen[1,2], Zhilong Huang[1*], Ruidong Yang[2], Lijuan Du[2], Wenchao Su[2], Lulin Zheng[3] & Lin Ye[1]

[1] *State Key Laboratory of Ore Deposit Geochemistry, Institute of Geochemistry, Chinese Academy of Sciences, Guiyang 550081, China;*
[2] *College of Resources and Environmental Engineering, Guizhou University, Guiyang 550025, China;*
[3] *Mining College of Guizhou University, Guiyang 550025, China*
* Corresponding author, E-mail: huangzhilong@vip.gyig.ac.cn

Carlin-type gold mineralization represents one of the world’s most important Au resources. Despite the many studies conducted in the past three decades, the gold sources and metallogenic dynamics remain enigmatic. Here, we report actively forming auriferous mounds and sulfide concretions from the Middle-Upper Permian basalt-dominated submarine volcanic-sedimentary rocks within the Carlin-style gold deposits, Youjiang basin, China. The volcanic-sedimentary rocks consist of basalt, tuff, scoria, black ash and metalliferous sediments in an unaltered sequence, which overlies the Middle Permian Maokou Formation and underlines by the Upper Permian strata. In this paper, we investigate the native gold nanoparticles in the volcanic-sedimentary rocks, and provide new insight into a new type of Au mineralization in the Youjiang basin. We unravel the mineralogy, trace elements and sulfur isotope compositions of these native gold and associated sulfides (e.g., marcasite and pyrite) via EPMA, *in-situ* LA-ICP-MS and NanoSIMS analyses. Petrographic obsevations show that native gold grains are present in marcasite microfractures, with sizes of 1 to 5 μm. The marcasites is interpreted to be of sedimentary exhalative (SEDEX) origin, as they are hosted by sulfide concretions comprising of sulfide-rich aggregates, quartz, barite, and basaltic tuff fragments. The EPMA elemental mapping suggests that the native gold grains have high contents of Hg, Cu, Zn and Sb, an ore elements assemblage common in typical Carlin-type Au mineralization (Au-As-Hg-Sb±Cu±Zn). LA-ICP-MS analysis shows the Au^0-bearing marcasite is featured by lower Co/Ni ratios (avg. = 0.12), relatively high Ti (mostly 39–890 ppm, some > 10000 ppm) and low Cu (1–32 ppm), As (1–920 ppm), Zn (0–5 ppm) and Au (0–0.53 ppm) contents. The low Co/Ni ratios and elevated Ti contents suggest that the marcasite was likely sedimentary and/or diagenetic process, which associated with high-Ti Emeishan basalt eruption in Middle-Late Permian. NanoSIMS analysis shows that the marcasite $\delta^{34}S$ varies from 20.30‰ to 34.29‰ (avg. = 25.86‰), indicating that thermochemical sulfate reduction (TSR) may have provided the sulfur under open system for sulfate but close for H_2S. Overall, this paper proposed that (1) the Middle-Upper Permian volcanic-sedimentary rocks enriched in Au-Sb-Hg±Cu±Zn probably formed the source-bed for the Carlin-gold mineralization in Yanshanian (~140 Ma); (2) significant amounts of gold can occur in the basalt-dominated SEDEX environment. In addition, the genetic relationship between Emeishan plume and Carlin-type gold mineralization is also discussed in this paper. Based on previous studies, the juvenile lower crust beneath the eastern Emeishan large igneous province (LIP) may have been a potential Au source, and the associated mantle underplating may have contributed to the formation of Carlin-style Au deposits. Therefore, we propose a possible genetic link between the Carlin-type mineralization and Emeishan LIP magmatism in the Youjiang basin. Our findings offer a new exploration target which is unaltered volcanic-sedimentary rocks in the Youjing basin, may have been a source of gold for the large-scale Carlin-style gold mineralization in Yanshanian (~140 Ma), and demonstrate that significant amounts of gold can occur in a basalt-dominated SEDEX environment.

native gold, sedimentary exhalative (SEDEX), Emeishan basalt, Carlin-type gold deposit, Youjiang basin

doi: 10.1360/TB-2019-0837